

# NMR-based conformational analysis of perezone and analogues

L. Gerardo Zepeda,<sup>a</sup> Eleuterio Burgueño-Tapia,<sup>a</sup> Nury Pérez-Hernández,<sup>b</sup> Gabriel Cuevas<sup>c</sup> and Pedro Joseph-Nathan<sup>d\*</sup>

Complete assignment of the <sup>1</sup>H NMR chemical shift and coupling constant values of perezone (**1**), O-methylperezone (**2**) and 6-hydroxyperezone (**3**) was carried out by total-line-shape-fitting calculations using the PERCH iterative spectra analysis software (PERCH Solutions Ltd., Kuopio, Finland). The resulting simulated spectra for the three compounds showed strong similarity to their corresponding experimental spectra. Particularly, all vicinal, allylic and homoallylic coupling constant values for the side chain of the three compounds were very similar, thus revealing that the conformation of these three molecules in solution is indeed almost identical. This fact is in agreement with extended side chain conformations over folded chain conformations because **1**, **2** and **3** undergo completely different intramolecular cycloaddition reactions. In addition, results of double pulsed field gradient spin echo NOESY 1D experiments performed on perezone (**1**) were unable to provide evidence for folded conformers. Copyright © 2013 John Wiley & Sons, Ltd.

**Keywords:** perezone; hydroxyperezone; O-methylperezone; pipitzol; <sup>1</sup>H NMR; iterative NMR spectral analysis; NOE

## Introduction

Since its discovery over 160 years ago,<sup>[1]</sup> perezone (**1**) has been the subject of a large number of studies because of its relative abundance in plants of the genus *Perezia* and its interesting biological and reactivity properties that originate a wide variety of natural and synthetic molecules.<sup>[2]</sup> Such structural diversity of perezone derivatives is closely related to both the chemical nature and the relative conformation of the side chain and the quinone ring. For instance, thermal transformation<sup>[3]</sup> of perezone (**1**) affords a 1 : 1 mixture (Figure 1) of  $\alpha$ -pipitzol (**4**) and  $\beta$ -pipitzol (**5**), whereas in the presence of F<sub>3</sub>B/OEt<sub>2</sub>, it yields a 9 : 1 mixture in favor<sup>[4]</sup> of the  $\alpha$ -isomer. This stereoselectivity was inverted<sup>[5]</sup> to a 1 : 3 mixture in favor of the  $\beta$ -isomer by treating methyl ether **2** with AlCl<sub>3</sub>/Et<sub>2</sub>S and further improved<sup>[6]</sup> to a 1 : 8 ratio by treating **2** with F<sub>3</sub>B/OEt<sub>2</sub>. In contrast, treatment of natural 6-hydroxyperezone (**3**) with F<sub>3</sub>B/OEt<sub>2</sub> followed a completely different course affording<sup>[7]</sup> the stable perezinone-BF<sub>2</sub> adduct (**6**).

From a mechanistic point of view, the thermal transformation of perezone (**1**) to  $\alpha$ -pipitzol (**4**) and  $\beta$ -pipitzol (**5**) was either proposed as a two-step Michael-type intramolecular cycloaddition<sup>[8]</sup> or rationalized by Woodward as a concerted cycloaddition involving a [1,9]-sigmatropic change of order.<sup>[8,9]</sup> The later reaction path was confirmed when the reaction was carried out using 15-deuteroperezone to afford  $\alpha$ -pipitzol (**4**) and  $\beta$ -pipitzol (**5**) labeled at only one methyl of the *gem*-dimethyl group of each compound.<sup>[3]</sup> Under the thermal reaction condition, no chiral induction by the sole stereogenic center of perezone (**1**) was evident. In turn, the structures of tricyclic natural occurring sesquiterpenes  $\alpha$ -pipitzol (**4**) and  $\beta$ -pipitzol (**5**) followed after extensive chemical degradation reactions,<sup>[10]</sup> which allowed determining the structure<sup>[11]</sup> of perezone (**1**), whereas their absolute configuration was established by optical rotatory dispersion measurements.<sup>[12]</sup> In addition, a single crystal X-ray diffraction study independently confirmed the structure of  $\alpha$ -pipitzol (**4**) and related molecules.<sup>[13]</sup>

Variable temperature <sup>13</sup>C NMR measurements<sup>[14]</sup> allowed to evaluate the fast interconversion of the two isoenergetic tautomers of 6-hydroxyperezone (**3**), which only could be slowed in the solid state as evidenced by CP-MAS measurements.<sup>[15]</sup>

A few years ago, a conformational study substantiated on NOE and cyclic voltammetry experiments<sup>[16]</sup> described the side chain of **1** adopts a folded conformation dominated by  $\pi$ - $\pi$  interactions between the side chain double bond and the quinone system. In this study, it was suggested that  $\pi$ - $\pi$  interactions are likely the driving force that controls some chemical properties of **1**, for instance, its predominant stereoselective conversion to  $\alpha$ -pipitzol (**4**), although the study ignored the transformation of O-methylperezone (**2**), which leads predominantly to  $\beta$ -pipitzol (**5**). These results were significantly different from the conclusion reached after exhaustive conformational analysis of perezone (**1**) required<sup>[17]</sup> for a vibrational circular dichroism study, which resulted in preferred extended side chain conformations.

\* Correspondence to: Pedro Joseph-Nathan, Departamento de Química, Centro de Investigación y de Estudios Avanzados del Instituto Politécnico Nacional, Apartado 14-740, México D.F., 07000 Mexico. E-mail: pjoseph@nathan.cinvestav.mx

a Departamento de Química Orgánica, Escuela Nacional de Ciencias Biológicas, Instituto Politécnico Nacional, Prolongación de Carpio y Plan de Ayala, Col. Santo Tomás, México, D.F., 11340, Mexico

b Escuela Nacional de Medicina y Homeopatía, Instituto Politécnico Nacional, Guillermo Massieu Helguera 239, Col. Residencial La Escalera, Mexico, D.F., 07320, Mexico

c Instituto de Química, Universidad Nacional Autónoma de México, Circuito Exterior, Ciudad Universitaria, D.F., 04510, Mexico

d Departamento de Química, Centro de Investigación y de Estudios Avanzados del Instituto Politécnico Nacional, Apartado 14-740, México, D.F., 07000, Mexico

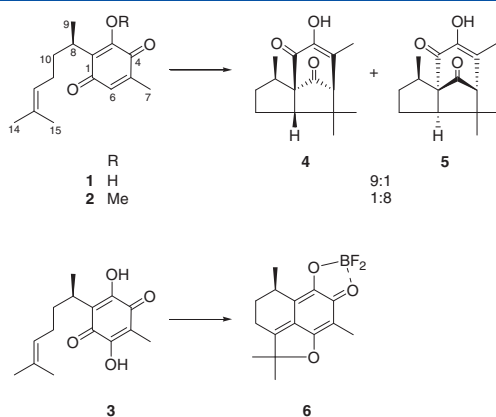


**Figure 1.** Chemical structures of compounds 1–6.

To complement the results of the conformational analysis described in these two works,<sup>[16,17]</sup> a complete NMR-based conformational analysis of perezone (**1**), its *O*-methyl derivative (**2**) and natural occurring hydroxyperezone (**3**) is described herein by comparison of experimental and calculated spectra obtained using the PERCH iterative NMR spectra analysis software (PERCH Solutions Ltd., Kuopio, Finland).

## Results and Discussion

As mentioned earlier, 5 years ago, it was proposed<sup>[16]</sup> that dispersion forces are responsible for maintaining the side chain and quinone ring of perezone (**1**) in close proximity. The resulting conformational arrangement was assumed presumably to be responsible for the conversion of **1** into  $\alpha$ -pipitzol (**4**) and  $\beta$ -pipitzol (**5**). Seeking to provide more information on the conformational preference of natural occurring perezone (**1**), a recent comparative vibrational circular dichroism (VCD) study of **1** and dihydroperezone, the derivative having the saturated side chain, yielded quite similar VCD spectra for both compounds, which comprise a large number of side chain extended conformers as followed after extensive density functional theory calculations.<sup>[17]</sup>

Evaluation of <sup>1</sup>H NMR coupling constants is a powerful tool to obtain conformational information. This goal can be achieved by using NMR simulation software, whose usefulness has recently been described in the field of natural products.<sup>[18–22]</sup> This analysis yields all NMR parameters ( $\delta$  and <sup>n</sup>J) of all hydrogen atoms in the target molecule and consists of an iterative minimization of the difference between the spin–spin simulated and experimental spectra.<sup>[23]</sup> Taking advantage of this tool, we have now completed a full analysis of the coupling constants for **1–3**. It includes assignment of the small allylic and homoallylic coupling constant values for the CH<sub>2</sub>(11)–CH(12)C(13)–[CH<sub>3</sub>(14)]CH<sub>3</sub>(15) fragment, as well as the  $\delta$  values owing to the individual signals of the C-10 and C-11 methylene groups. The spin system analysis was started by individual assignment of the hydrogen atoms of the methylene groups. Selective irradiation of the H-8 signal ( $\delta$  3.050) of **1** caused a loss of scalar coupling in the signals at  $\delta$  1.805 and 1.581, assigning them to the hydrogen atoms of the CH<sub>2</sub>-10 group. The overlapped CH<sub>2</sub>-11 signals were observed as a complex multiplet centered at  $\delta$  1.890 as a result of vicinal coupling with CH<sub>2</sub>-10 and H-12, as well as homoallylic couplings with the C-14 and C-15 methyl groups. Once the vicinal and allylic coupling constant values were known, the remaining assignments were assisted by homonuclear irradiations.

The 500 MHz <sup>1</sup>H NMR FID of perezone (**1**) was Fourier transformed into the frequency domain spectrum using the PERCH preparation module. The molecular model for **1** was used to predict and generate a preliminary calculated <sup>1</sup>H NMR spectrum of the molecule. Before iteration, all chemical shift and vicinal coupling constant values obtained from the experimental spectrum were manually adjusted and submitted to the iterator module using the total-line-shape-fitting method. After successive trials, the best solution showed a root-mean-square (RMS) error of 0.057%. Full <sup>1</sup>H NMR spin data of **1** are shown in Table 1, and experimental and simulated <sup>1</sup>H NMR spectra are compared in Figure 2.

Although PERCH calculation provide chemical shift values with six significant figures, because the experimental 500 MHz NMR spectra were acquired with a resolution better than 0.4 Hz, the chemical shifts given in Table 1 with three digits after the decimal point constitute a proper description. The table also reports PERCH-derived *J* values with two figures after the decimal point, as in similar cases.<sup>[20,21]</sup> The software also provides automatic distinction of the *pro-R* and *pro-S* signals owing to the hydrogen atoms at C-10 and C-11.

A molecular model of *O*-methylperezone (**2**), which in contrast to **1**, in the presence of F<sub>3</sub>B/OEt<sub>2</sub> affords **5** as the main product, was constructed and used to generate the initial calculated spectrum. After manual adjustment of the chemical shift and coupling constant values, the spectrum was repeatedly iterated as in the previous case. The best solution showed an RMS error of 0.058%

**Table 1.** Complete <sup>1</sup>H NMR spin–spin analysis of **1–3** (15 mg) in CDCl<sub>3</sub> (1 ml) at 500 MHz and 298 K; Chemical shifts are in ppm from TMS, and coupling constants are in Hz.

Atom	<b>1</b>	<b>2</b>	<b>3</b>
H-7	2.056	2.008	1.933
H-8	3.050	3.074	3.028
H-9	1.198	1.172	1.203
H-10 <sub>R</sub>	1.805	1.728	1.793
H-10 <sub>S</sub>	1.581	1.573	1.581
H-11 <sub>R</sub>	1.864	1.840	1.919
H-11 <sub>S</sub>	1.921	1.910	1.879
H-12	5.077	5.043	5.060
H-14	1.644	1.635	1.646
H-15	1.536	1.527	1.533
<i>J</i> <sub>8,9</sub>	7.08	7.06	7.07
<i>J</i> <sub>8,10<sub>R</sub></sub>	8.87	8.63	9.29
<i>J</i> <sub>8,10<sub>S</sub></sub>	6.50	6.68	6.67
<i>J</i> <sub>10<sub>R</sub>,10<sub>S</sub></sub>	–13.21	–13.25	–13.49
<i>J</i> <sub>10<sub>R</sub>,11<sub>R</sub></sub>	5.97	6.07	5.52
<i>J</i> <sub>10<sub>R</sub>,11<sub>S</sub></sub>	9.37	9.37	9.40
<i>J</i> <sub>10<sub>S</sub>,11<sub>S</sub></sub>	6.23	6.17	6.20
<i>J</i> <sub>10<sub>S</sub>,11<sub>R</sub></sub>	9.41	9.47	9.05
<i>J</i> <sub>11<sub>R</sub>,11<sub>S</sub></sub>	–14.09	–14.33	–14.72
<i>J</i> <sub>11<sub>R</sub>,12</sub>	7.17	7.25	6.91
<i>J</i> <sub>11<sub>S</sub>,12</sub>	7.05	6.90	7.28
<i>J</i> <sub>11<sub>R</sub>,14</sub>	1.22	1.23	1.32
<i>J</i> <sub>11<sub>S</sub>,14</sub>	1.20	1.21	1.20
<i>J</i> <sub>11<sub>R</sub>,15</sub>	0.82	0.78	0.83
<i>J</i> <sub>11<sub>S</sub>,15</sub>	0.00	0.00	0.00
<i>J</i> <sub>12,14</sub>	1.41	1.38	1.33
<i>J</i> <sub>12,15</sub>	1.39	1.38	1.39
RMS(%)	0.057	0.058	0.058
RMS, root-mean-square.			

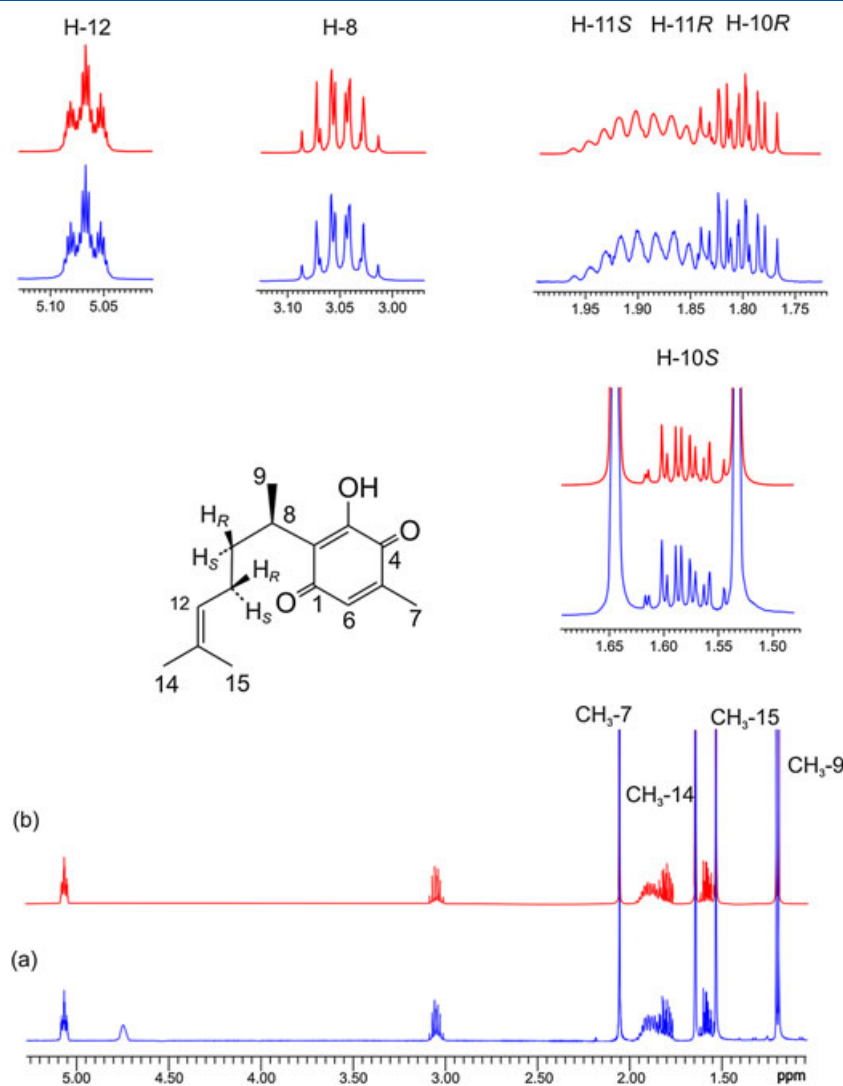


**Figure 2.** Comparison of experimental (a) and PERCH calculated (b) 500 MHz  $^1\text{H}$  NMR spectra of perezone (**1**) and expansions of specific regions.

(Table 1), and experimental and simulated spectra are compared in Figure 3.

Finally, natural 6-hydroxyperezone (**3**), which under similar  $\text{F}_3\text{B}/\text{OEt}_2$  reaction condition only affords adduct **6**, was treated as earlier. After manual adjustment of the chemical shift and coupling constant values and iteration of the initial calculated spectrum, the chemical shift and coupling constant values shown in Table 1, with an RMS error of 0.058%, were obtained. The corresponding experimental and simulated spectra are shown in Figure 4. As can be seen in Table 1, coupling constant values for the side chain of **1–3** are quite similar, suggesting the conformational arrangement of **1–3** to also be very similar. The  $J$  values for the  $\text{CH}_2(11)\text{--CH}(12)\text{C}(13)[\text{CH}_3(14)]\text{--CH}_3(15)$  fragment of **1–3** are also similar to those of leubethanol, a tetraline diterpene having the same side chain.<sup>[20]</sup>

According to published results,<sup>[16]</sup> evidence for  $\pi\text{--}\pi$  interaction between the side chain and the quinone ring of perezone (**1**) was obtained through NOE measurements using the double pulsed field gradient spin echo NOE technique. Thus, after selective inversion of the Me-15 group, NOE on H-6 (0.6–0.8%) and Me-7 (0.4–0.5%) were reported.<sup>[16]</sup> Therefore and in search to find experimental support, we used the same pulse sequence that is

the most appropriate one for measuring weak dipolar interactions in small molecules.<sup>[24]</sup> After careful calibration of acquisition parameters to minimize the presence of artifacts (Experimental section), a series of NOESY 1D experiments were measured by selective inversion of those representative hydrogen atoms, which could provide information about a possible  $\pi\text{--}\pi$  interaction between the double bond and the quinone ring of **1**.

In the case of the quinone ring, selective inversion of the H-6 signal caused a 2.0% enhancement of the Me-7 signal, whereas inversion of the Me-7 signal caused 0.7% enhancement of the H-6 signal. In neither case were enhancements on the H-12, Me-14 or Me-15 signals observed. The signals owing to the side chain behave similarly. Inversion of the H-12 signal caused a 1.9% enhancement of the Me-14 signal, inversion of Me-14 caused 0.8% and 1.0% enhancements of H-12 and Me-15, respectively, and inversion of Me-15 caused 1.2% enhancement of Me-14. Again, in neither case could NOE be detected on the H-6 or Me-7 signals.

According to the aforementioned results, it seems evident NOE experiments are not providing reliable evidence concerning  $\pi\text{--}\pi$  interactions because they could be too weak or take place as a fast process not detectable in the NMR time scale of dipolar interactions. In other words, conversion of perezone (**1**) into pipitzols

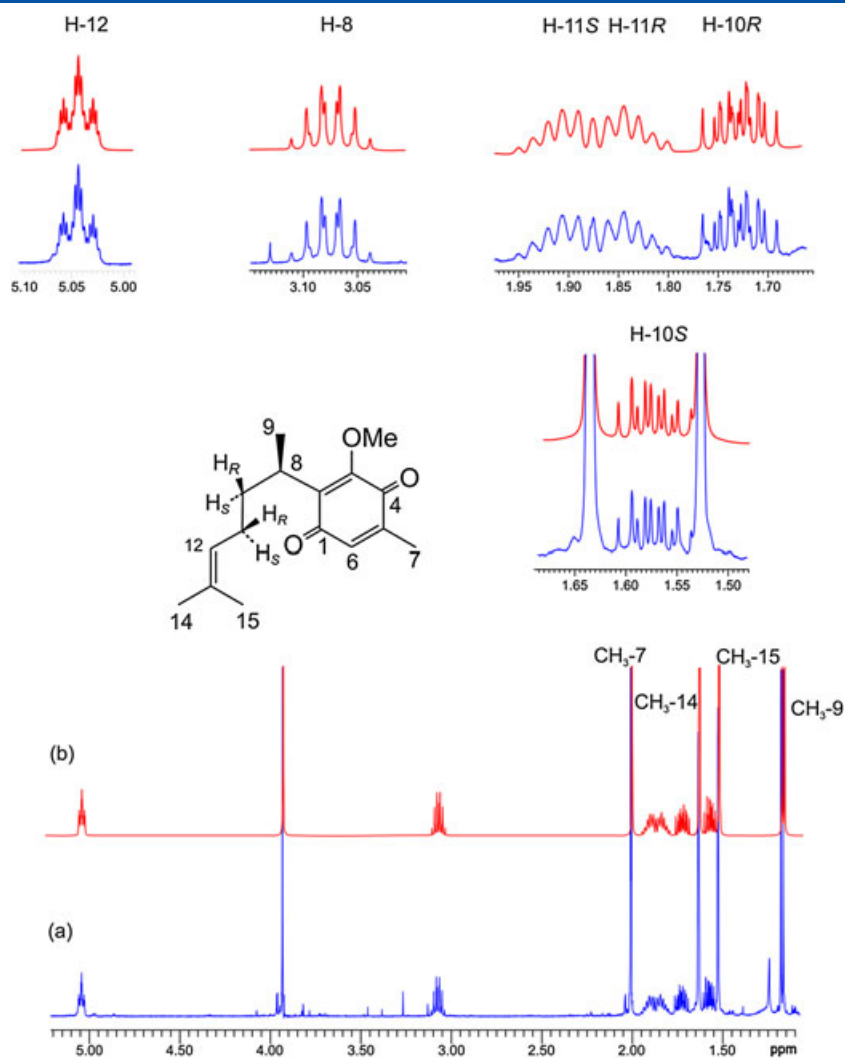


**Figure 3.** Comparison of experimental (a) and PERCH calculated (b) 500 MHz  $^1\text{H}$  NMR spectra of *O*-methylperezone (**2**) and expansions of specific regions.

inevitably involves a close approach of the side chain to the quinone ring, likely mediated by a  $\pi$ - $\pi$  interaction that must be reached at the transition state level whose energy is provided by the reaction conditions. At room temperature, this interaction seems negligible to be detected by NOE experiments.

In conclusion, complete  $^1\text{H}$  NMR spectral analysis of perezone (**1**), *O*-methylperezone (**2**) and 6-hydroxyperezone (**3**) was achieved with the aid of PERCH software. The RMS deviation between experimental and simulated spectra for **1–3** was less than 0.06%. The coupling constant values for the side chain  $^1\text{H}$  NMR signals are quite similar, from where it might be concluded that the conformation of these three compounds in solution is essentially the same. In addition, NOESY 1D experiments were unable to find evidence supporting  $\pi$ - $\pi$  interaction between the side chain and the quinone ring of perezone (**1**).

## Experimental

### Compounds

Perezone (**1**), *O*-methylperezone (**2**) and 6-hydroxyperezone (**3**) were available from a pioneering continuous-wave  $^{13}\text{C}$  NMR study.<sup>[25]</sup>

### $^1\text{H}$ NMR full spin-spin analysis

$^1\text{H}$  NMR spectra of **1–3** were recorded on a Varian VNMRS 500 spectrometer (Varian Associates, Palo Alto, CA, USA) in  $\text{CDCl}_3$  solutions using a magnet homogeneity better than 0.4 Hz operated at 298 K. PERCH NMR software was employed for spin-spin system analysis, starting with the generation of the frequency domain  $^1\text{H}$  NMR spectra from the 500 MHz FIDs in the preparation module. The construction of molecular models for **1–3** was carried out to obtain the initial calculated spectra. Previous to iteration, some coupling constant and chemical shift values extracted from the experimental spectra were manually fitted into the calculation package, and then the calculated spectra of **1–3** were repeatedly submitted to iterations using the total-line-shape-fitting mode.

### NOESY 1D experiments

All NOESY 1D experiments were performed at 299 K on a Varian VNMRS 500 MHz spectrometer equipped with a OneNMR 5 mm probe and an actively shielded Z-gradient coil. The double pulsed field gradient spin echo experiment was implemented through the pulse sequence NOESY1D\_zqf3 with ZQ filter. A sample of 20 mg of perezone was dissolved in 0.9 ml of  $\text{CDCl}_3$  and degassed

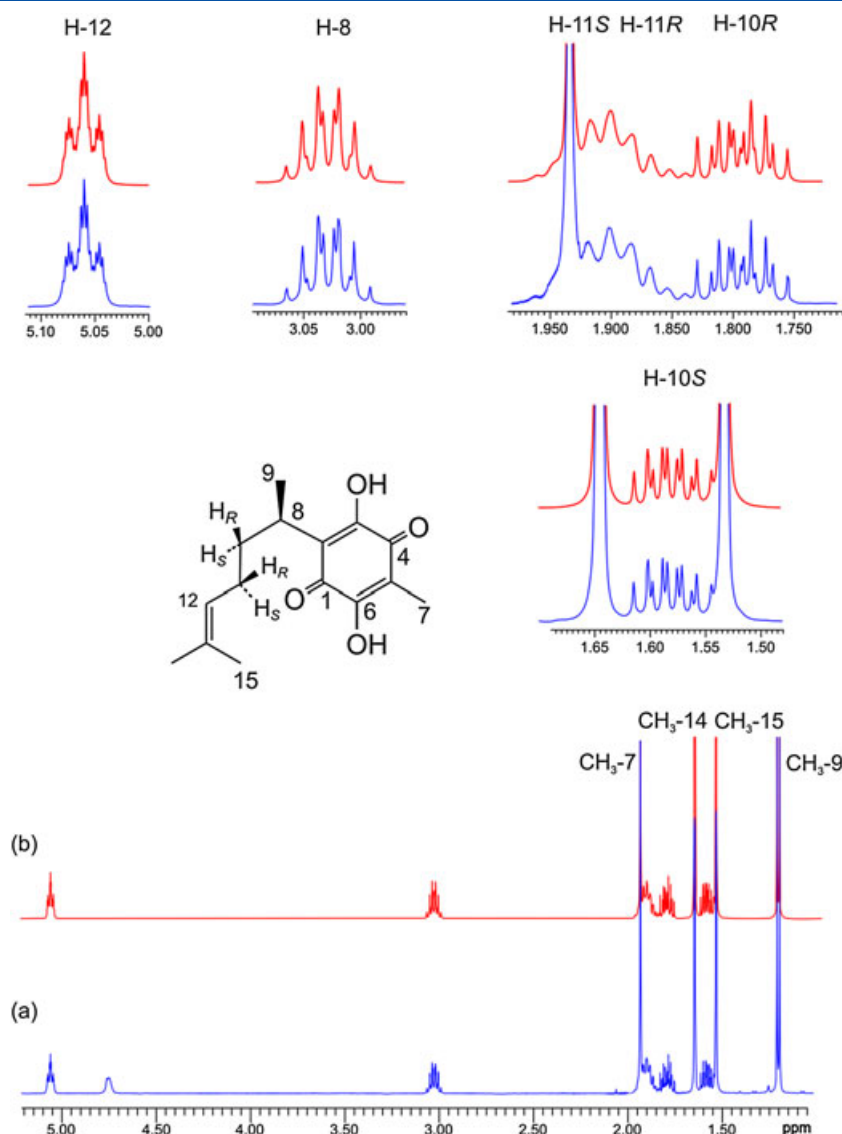


**Figure 4.** Comparison of experimental (a) and PERCH calculated (b) 500 MHz  $^1\text{H}$  NMR spectra of 6-hydroxyperezone (**3**) and expansions of specific regions.

with simultaneous slow bubbling of Ar and ultrasound during 25 min. A final volume of 0.7 ml of  $\text{CDCl}_3$  was left. After calibration of the  $90^\circ$  pulse width ( $10.9\ \mu\text{s}$ , power transmitter attenuation = 58), the following acquisition parameters were used: pre-acquisition delay, 1 s; number of transients, 512; acquisition time, 2 s; Fourier number, 32k-data; and spectral width, 8012.8 Hz. After recording a series of arrayed experiments in the range  $\tau_{\text{mix}} = 0.0\text{--}1.0\ \text{s}$ , an optimum mixing time ( $\tau_{\text{mix}}$ ) of 0.8 s was found.

### Acknowledgement

Partial financial support from Conacyt-México, grant 152994, is acknowledged.

### References

- [1] L. Río de la Loza, Discurso pronunciado por el catedrático de química médica de la Escuela de Medicina (November 23, 1852), in *Escritos de Leopoldo Río de la Loza*, (Ed.: J. M. Noriega compiler), Imprenta de Ignacio Escalante, México, **1911**, 94–100.
- [2] P. Joseph-Nathan, R. L. Santillan, in *Studies in Natural Products Chemistry. Structural Elucidation (Part B) vol. 5*. (A.-u. Rahman Ed.), Elsevier, Amsterdam, **1989**, 763–813.
- [3] P. Joseph-Nathan, V. Mendoza, E. García. *Tetrahedron* **1977**, *33*, 1573–1576.
- [4] I. H. Sánchez, R. Yañez, R. Enríquez, P. Joseph-Nathan. *J. Org. Chem.* **1981**, *46*, 2818–2819.
- [5] I. H. Sánchez, F. Basurto, P. Joseph-Nathan. *J. Nat. Prod.* **1984**, *47*, 382–383.
- [6] P. Joseph-Nathan, E. Burgueño-Tapia, R. L. Saltillan. *J. Nat. Prod.* **1993**, *56*, 1758–1765.
- [7] P. Joseph-Nathan, M. E. Garibay, R. L. Saltillan. *J. Org. Chem.* **1987**, *52*, 759–763.
- [8] E. R. Wagner, R. D. Moss, R. M. Brooker, J. P. Heeschen, W. J. Potts, M. L. Dilling, *Tetrahedron Lett.* **1965**, *6*, 4233–4239.
- [9] R. B. Woodward, R. Hoffmann, *The Conservation of Orbital Symmetry*, Academic Press, New York, **1970**, pp. 87.
- [10] F. Walls, J. Padilla, P. Joseph-Nathan, F. Giral, J. Romo, *Tetrahedron Lett.* **1965**, *6*, 1577–1582.
- [11] F. Walls, M. Salmón, J. Padilla, P. Joseph-Nathan, J. Romo. *Bol. Inst. Quím. Univ. Nat. Autón. Méx.* **1965**, *17*, 3–15.
- [12] F. Walls, J. Padilla, P. Joseph-Nathan, F. Giral, M. Escobar, J. Romo. *Tetrahedron* **1966**, *22*, 2387–2399.
- [13] P. Joseph-Nathan, L. U. Román, J. D. Hernández, Z. Taira, W. H. Watson, *Tetrahedron* **1980**, *36*, 731–734.

- [14] P. Joseph-Nathan, D. Abramo-Bruno, D. A. Ortega. *Magn. Reson. Chem.* **1981**, *15*, 311–316.
- [15] P. Joseph-Nathan, E. Martínez, M. Rojas, R. L. Santillan. *J. Nat. Prod.* **1987**, *50*, 860–865.
- [16] G. Roura-Pérez, B. Quiróz, M. Aguilar-Martínez, C. Frontana, A. Solano, I. González, J. A. Bautista-Martínez, J. Jiménez-Barbero, G. Cuevas. *J. Org. Chem.* **2007**, *72*, 1883–1894.
- [17] E. Burgueño-Tapia, C. M. Cerda-García-Rojas, P. Joseph-Nathan. *Phytochemistry* **2012**, *74*, 190–195.
- [18] M. Niemitz, R. Laatikainen, S.-N. Chen, R. Kleps, A. P. Kozikowski, G. F. Pauli. *Magn. Reson. Chem.* **2007**, *45*, 878–882.
- [19] J. M. Scher, A. Schinkovitz, J. Zapp, J. Wang, S. G. Franzblau, H. Becker, D. C. Lankin, G. F. Pauli. *J. Nat. Prod.* **2010**, *73*, 656–663.
- [20] G. M. Molina-Salinas, V. M. Rivas-Galindo, S. Said-Fernández, D. C. Lankin, M. A. Muñoz, P. Joseph-Nathan, G. F. Pauli, N. Waksman. *J. Nat. Prod.* **2011**, *74*, 1842–1850.
- [21] M. A. Muñoz, N. Pérez-Hernández, M. W. Pertino, G. Schmeda-Hirschmann, P. Joseph-Nathan. *J. Nat. Prod.* **2012**, *75*, 779–783.
- [22] J. G. Napolitano, D. C. Lankin, S. N. Chen, G. F. Pauli. *Magn. Reson. Chem.* **2012**, *50*, 569–575.
- [23] R. Laatikainen, M. Niemitz, U. Weber, J. Sundelin, T. Hassinen, J. Vepsäläinen. *J. Magn. Reson. Series A* **1996**, *120*, 1–10.
- [24] D. Neuhaus, M. Williamson, *The Nuclear Overhauser Effect in Structural and Conformational Analysis*, Wiley-VCH, New York, **2000**, pp. 258–279.
- [25] P. Joseph-Nathan, M. P. González, L. F. Johnson, J. N. Shoolery. *Magn. Reson. Chem.* **1971**, *3*, 23–29.